Morphology and Collapse Transitions in Binary Phospholipid Monolayers

Ajaykumar Gopal and Ka Yee C. Lee*

Department of Chemistry and Institute for Biophysical Dynamics, The University of Chicago, Chicago, Illinois

Received: July 3, 2001; In Final Form: August 13, 2001

We have concurrently studied the microscopic phase behavior, morphology, and surface pressure−area isotherms of Langmuir monolayers of a 7:3 mixture of DPPC (dipalmitoylphosphatidylcholine) and POPG (palmitoyloleoylphosphatidylglycerol) at various temperatures between 20 and 40 °C. The manner in which the monolayer, under compression, explores the third dimension at monolayer collapse correlates with the monolayer morphology prior to collapse. At temperatures below 28 °C, the monolayer is biphasic and collapses by forming large-scale folds, which reliably unfold upon expansion. These folded structures can be five to several hundred micrometers wide and up to millimeters long. Above 33.5 °C, the monolayer is homogeneous and, upon further compression, prefers to collapse through micron-scale vesicular structures that are globular or tubular in shape. Collapse occurs via both folding and vesiculation at temperatures between 28 and 33.5 °C, leading to the coexistence of the monolayer with both folds and vesicles. Analogous to equilibrium phase transitions, there may exist a temperature in this range, that can be thought of as a "triple point" temperature for the coexistence of the three "phases" corresponding to the two-dimensional monolayer, three-dimensional folds, and three-dimensional vesicles. In addition to this "triple point", the monolayer collapse mode is found to be independent of the path taken in the temperature−pressure parameter plane. The transition between the collapse modes thus resembles an equilibrium first-order phase transition.

Introduction

Langmuir monolayers have been extensively studied as biological membrane models[1] and widely used in materials as Langmuir−Blodgett (LB) films.[2] Phospholipid monolayers are of particular interest as in vitro models for cell membranes and other phospholipid-rich natural surfactant systems such as those in the lungs,[3] eyes,[4] and ears.[5,6]

The thermodynamic properties of Langmuir monolayers are primarily studied using surface pressure (Π)[7]−area (*A*) isotherms[8] obtained by monitoring Π as a function of the lateral compression of the film. Reduction in the area available to the molecules at the air−water interface causes a series of two-dimensional (2D) phase transformations.[1,9−14] At low surface density, the molecules at the interface are in a 2D gaslike (G) state. Increase in surface density by lateral compression of the monolayer leads to the transformation of the G phase into an isotropic 2D fluid phase called the liquid expanded (LE) phase. On further compression, the monolayer undergoes a transition from the uniform LE phase into the anisotropic condensed (C) phase by a first-order transition. Further compression of the C phase leads to transitions to different ordered phases similar to those found in liquid crystals.[15] Reduction in area beyond the equilibrium spreading pressure (ESP)[8,16] drives the monolayer into a metastable state from which it relaxes by the nucleation and growth of three-dimensional (3D) structures.[17,18] This 2D to 3D relaxation phenomenon is referred to as collapse, and the surface pressure at which this occurs is termed the collapse pressure (Π_c). Collapse causes 3D defects and discontinuities in the 2D monolayer and thereby determines the resultant morphology of the overcompressed film.

The formation of 3D discontinuities and defects in 2D monolayers adversely affects the fabrication of well-ordered

multilayered structures such as LB films[19] by disrupting the homogeneity and integrity of the monolayer. The coexistence of 2D and 3D structures, on the contrary, may be essential for the functioning of natural systems such as lung surfactant (LS).[20] It is thought that the coexistence of 3D reservoirs and 2D monolayers of lung surfactant material at the aqueous−air interface in the lungs allows efficient cycling of material in response to the periodic increases and decreases in interfacial area associated with breathing.[20] A deeper understanding of monolayer collapse phenomena, therefore, is essential in order to understand the workings of complex natural surfactant systems, and for tailoring defect-free and ordered monolayer or multilayer materials.

Fluorescence microscopy (FM),[12,21−23] Brewster angle microscopy,[24−27] scanning probe microscopy,[28−31] and light scattering microscopy[32] are widely used to characterize monolayers in terms of their 2D phase transformations and morphology at the nm-to-μm length scale. As outlined below, the use of these techniques to investigate monolayer collapse phenomena has yielded a wealth of information about various lipid systems. Light scattering microscopy experiments[33] show that a DPPC monolayer nucleates disklike 3D structures from the monolayer beyond the ESP and these grow and detach from the monolayer upon overcompression. Recent electron microscopy of DPPC films adsorbed at the air−water interface from lipid solutions suggests the formation of nanometer-scale vesicles and folds as potential modes of 3D relaxation of the monolayer.[34] Lipp and co-workers have recently shown by FM that DPPG (dipalmitoylphosphatidylglycerol) monolayers undergo a 2D−3D transition, which is more reversible than vesicle formation and of larger length scale (100 μm−1 mm).[35] Saint-Jalmes and co-workers have shown evidence for buckling of monolayers,[36] and other workers for the formation of more than one type of collapse structure as supported by a nucleation−growth−collision model.[37−39] Using surface pressure−area isotherms,

* Corresponding author. Phone: (773) 703-7068. Fax: (773) 702-0805. E-mail: kayeelee@uchicago.edu.

Monolayer Collapse Transitions

J. Phys. Chem. B, Vol. 105, No. 42, 2001 **10349**

Lundquist showed that the mode of collapse in alkyl esters was dependent on the temperature of the system.[40]

The dependence of monolayer collapse on macroscopic parameters such as temperature and monolayer compression rate,[40,41] and microscopic factors such as intermolecular interactions, nucleation, growth rate of nuclei,[18] lipid head–tail asymmetry,[42] and monolayer thickness[36] has evoked different theoretical models to explain often-disparate experimental observations. Very few experiments and models, however, deal with the interplay between the macroscopic and microscopic properties of the monolayer that determine collapse behavior. In this work, we investigate the effect of phase equilibrium on the morphology of the film and how this may determine the length scale and mode of monolayer collapse. Using binary phospholipid monolayers as experimental evidence, we propose a qualitative model (quantitatively detailed elsewhere[43,44]) for the interplay between monolayer phase equilibrium, morphology, and collapse mode.

Natural bilayer membranes[45] and monolayers[46] usually occur as complex heterogeneous mixtures of phospholipids and proteins. The heterogeneity is typically attributed to phase separation of the lipid components in the mixture. There is direct experimental evidence of phase separation, for example, in monolayers of model lung surfactant lipids[47–49] as well as lipid bilayers.[50,51] The binary lipid system chosen for this study is a 7:3 mixture of DPPC (dipalmitoylphosphatidylcholine) and POPG (palmitoyloleoylphosphatidylglycerol), both of which are components of natural lung surfactant.[52] It has been reported that the critical temperature for phase separation for a 7:3 mixture of DPPC and egg phosphatidylglycerol (egg PG) is 33 °C.[53] DPPC monolayers are known to pack into a condensed phase and attain near-zero surface tension at high compression. POPG, on the other hand, is an unsaturated phospholipid that does not pack well, and is believed to act as the "fluidizing" minor component in LS. Using temperature as a handle to alter the phase equilibrium and thus the morphology of the monolayer, we have used FM to probe the corresponding changes in the mode of 2D–3D collapse transition. We find a strong correlation between the temperature-dependent morphology of the monolayer and its 2D–3D transition behavior.

Experimental Methods

Lipids and Subphase. Solid DPPC and ampules of POPG in chloroform were both obtained from Avanti Polar Lipids, Inc (Alabaster, AL). They were diluted with chloroform (HPLC grade, Fisher Scientific, Pittsburgh, PA), and mixed in a molar ratio of 7:3, respectively, to obtain a spreading solution of concentration 0.1 mg mL^{-1}. One mole % of Texas Red 1,2-dihexadecanoyl-*sn*-glycero-3-phosphoethanolamine, triethylammonium salt (Molecular Probes Inc., Eugene, OR) was the fluorescent probe used. The subphase used for all the experiments was ultrapure water (resistivity $\geq$ 18 MΩ cm) made using a combination of reverse osmosis and ultra-purification (RiOs/Elix-10 and Milli-Q, Millipore, Bedford, MA).

Instrumental Setup. Surface pressure (Π)–area (A) isotherms are obtained using a home-built Langmuir trough[21,22] by monitoring the surface pressure with a Wilhelmy surface balance (Reigler & Kirstein, Berlin, Germany) as the surface area is reduced (compression) or increased (expansion). In the case of binary mixtures, the area plotted in the isotherms represents the mean area per phospholipid molecule. The apparatus consists of a Teflon trough (27.5 cm × 6.25 cm × 0.63 cm) fitted with two symmetrically mobile barriers (l = 6.25 cm) made of the same material and a filter-paper strip used

as the surface balance probe. The maximum working surface area is 145 cm^2. All the isotherm data presented here have been collected at a linear compression rate of 0.1 mm s^{-1}. Depending on the initial amount of material deposited at the interface, this translates to a molecular area reduction rate between 0.04 and 0.06 Å^2 s^{-1}. The temperature of the water subphase is maintained within 0.5 °C of the target temperature using a home-built control assembly consisting of thermoelectric units (Omega Engineering Inc, Stamford, CT) attached to a heat sink maintained at 20 °C by a Neslab RTE-100 water circulator (Portsmouth, NH). The trough is kept covered with a resistively heated indium tin oxide coated glass plate (Delta Technologies, Dallas, TX), which is maintained at approximately 2 °C above the target subphase temperature in order to minimize air currents, reduce evaporative losses, and prevent condensation of water on the microscope objective.

The Langmuir trough sits on translation stages that allow for scanning of the air–water interface in *x*, *y,* and *z* directions. The entire assembly is in turn fitted on a custom microscope stage for concurrent fluorescence microscopy with a 50× extra-long working distance objective lens (Nikon Y-FL, Fryer Co., Huntley, IL). The filter cube (Nikon HYQ Texas Red, Fryer Co., Huntley, IL) used permits excitation between 530 and 590 nm and emission between 610 and 690 nm. A silicon intensified target (SIT) camera (Hamamatsu Corporation, Bridgewater, NJ) is used to collect video rate (30 frames/s) images, which are recorded on Super-VHS (S-VHS) format videotape with an appropriate recorder (JVC HR-S4500U, JVC Co. of America, Wayne, NJ). This arrangement allows the microscopic morphology of the monolayer to be examined over a large lateral area while concurrent isotherm data are collected.

The entire assembly above is mounted on a vibration isolation table (Newport, Irvine, CA) and controlled completely by a custom software interface written using LabView 4.1 (National Instruments, Dallas, TX).

Isothermal Compression Measurements. For each experiment, the subphase was first heated to the desired temperature, and the surface balance was calibrated to the value of surface tension of pure water for that temperature.[54] For all experiments, the volume of the subphase was maintained at 95 mL. The monolayer material was then spread at the interface and allowed to equilibrate for a period of 10 min. The barrier compression was started and isotherm data as Π (mN m^{-1}) vs A (Å^2 molecule^{-1}) were gathered automatically at 1-second intervals until the compression of the monolayer to collapse and subsequent expansion to near zero Π was complete. During this entire period, FM images were recorded on S-VHS tape as described earlier.

Heating Measurements. For experiments involving heating of the monolayer and subphase, the temperature was maintained at 25 °C while the monolayer was compressed to the surface pressure at which collapse was observed. The barriers were then switched from a linear compression mode to a computerized feedback mode, where Π was held constant by changing A. Constant pressure was maintained while the system was heated to 40 °C. FM images were recorded during the process as described earlier.

Image Grabbing and Handling. The images presented here were grabbed from the S-VHS tape as 640 pixel × 480 pixel bitmap images (BMP) using an 8 MB All-in-Wonder Pro Card (ATI Technologies, Thornhill, ON, Canada). The images were resized and enhanced in contrast and brightness within reasonable limits to make the features discernible for the purpose of display. The same amount of enhancement was not used for all
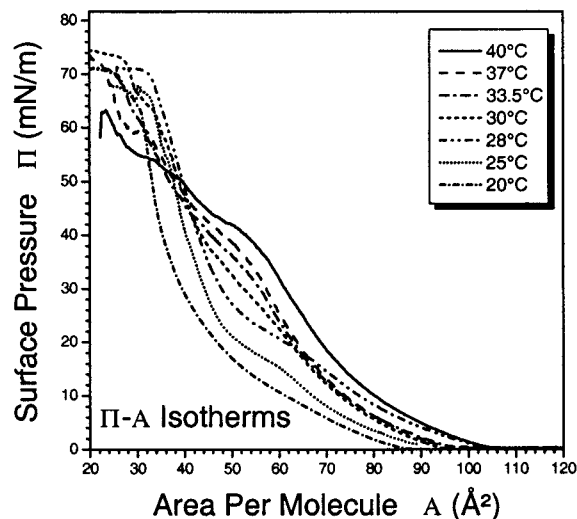
Figure 1. Overlay plot of surface pressure (Π) vs mean molecular area (A) for monolayers of 7:3 DPPC:POPG at temperatures ranging from 20 to 40 °C.

pictures; varying compensations were made to accommodate for the decrease in overall fluorescence intensity caused by photobleaching and nonradiative dye quenching at high molecular packing density.

Results

Surface pressure (Π) vs area (A) isotherms were measured for the 7:3 DPPC:POPG mixture with concurrent fluorescence microscopy at 20, 25, 28, 30, 33.5, 37, and 42 °C.

Isotherms and Phase Transitions. Figure 1 shows the overlay of isotherms measured at temperatures between 20 and 40 °C. All isotherms lift-off at molecular areas between 85 and 105 Å^2, indicating the emergence of a uniform LE phase from the G−LE coexistence. At 20 °C, the system is close to the triple point where the G, LE, and C phases coexist and, hence, the C phase nucleates in the presence of G and LE phases (morphology data not shown). This is manifested as a difference in the line shape of the 20 °C isotherm from the typical LE−C coexistence plateaus[55] seen for monolayers at 25 and 28 °C at molecular areas between 50 and 65 Å^2. The plateau is greatly reduced at 30 °C and disappears at 33.5 °C. FM images of the monolayer morphology (discussed later) indeed show no discernible phase separation beyond this temperature. The nucleation of collapse structures takes place close to 70 mN m^{-1} for monolayer temperatures between 20 and 30 °C and ranged from 45 to 60 mN m^{-1} for temperatures in the 33.5 to 40 °C range.

Monolayer Morphology and Collapse Modes. FM images of monolayer compression at 25, 30, and 37 °C are presented to provide insight into phase separation, domain morphology, and collapse structure. Figure 2 shows an isotherm for a 7:3 DPPC:POPG monolayer at 25 °C and FM images of the monolayer morphology at four points along the isotherm (Figure 2a−d). Figures 3 and 4 similarly show the isotherms and morphology of 7:3 DPPC:POPG monolayers at 30 and 37 °C, respectively.

At 25 °C, compression of the monolayer, initially in the G−LE coexistence, led to a uniform LE phase (Figure 2a). Further compression of the monolayer resulted in the nucleation and growth of C phase domains (Figure 2b) between 45 and 60 Å^2 per molecule. The LE−C biphasic domain structure (Figure 2c) was retained until the point of collapse as reported in other
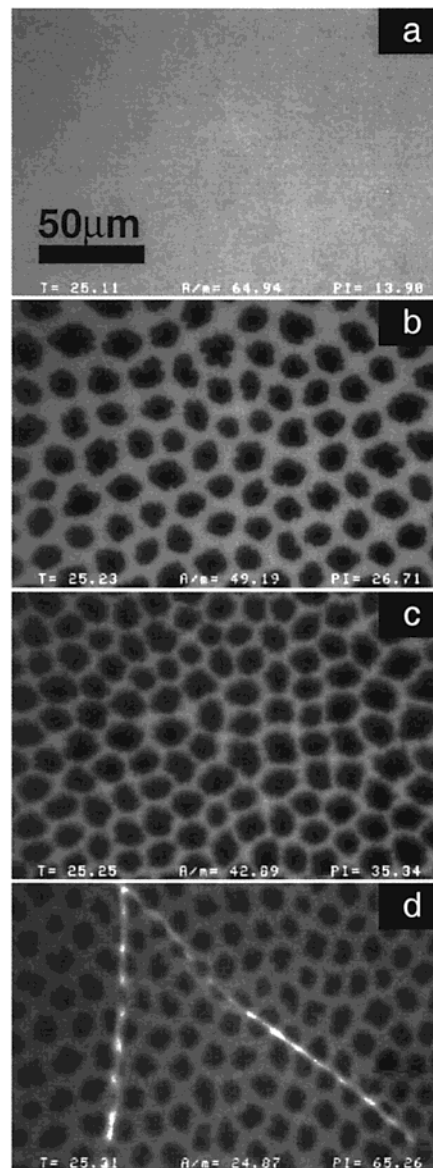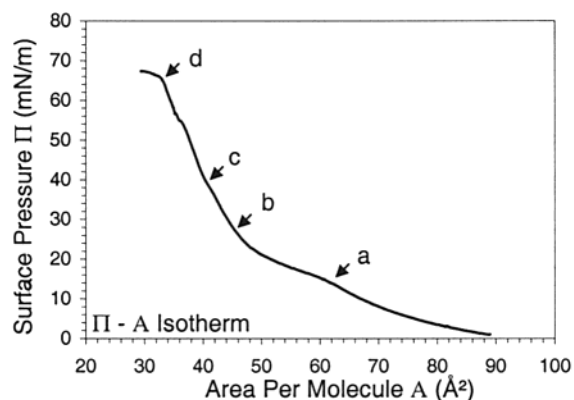

Figure 2. Isotherm for a 7:3 DPPC:POPG monolayer on pure water at 25 °C and FM images taken at various points along the isotherm − (a) the monolayer in a homogeneous LE phase; (b) the monolayer exhibits a biphasic morphology at the end of the plateau, with the dark domains being the condensed phase and the bright background the disordered LE phase; (c) fuzzy-edged condensed domains are sometimes observed due to domain boundary instabilities;[43] (d) large 100 μm scale folds are observed as bright streaks.

phospholipid monolayers.[56] The predominant mechanism of collapse was through reversible folding of the biphasic monolayer, which nucleated between 68 and 72 mN m^{-1} (Figure 2d).

Monolayer Collapse Transitions

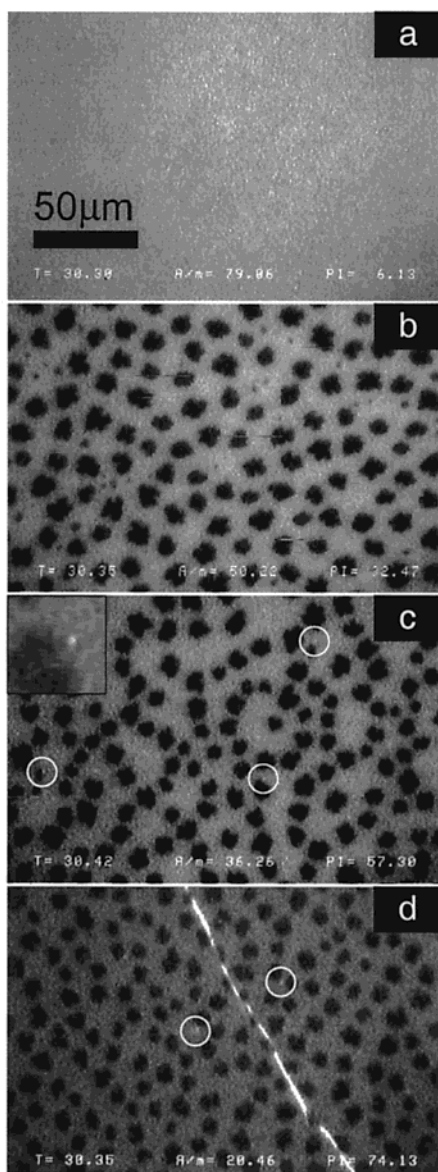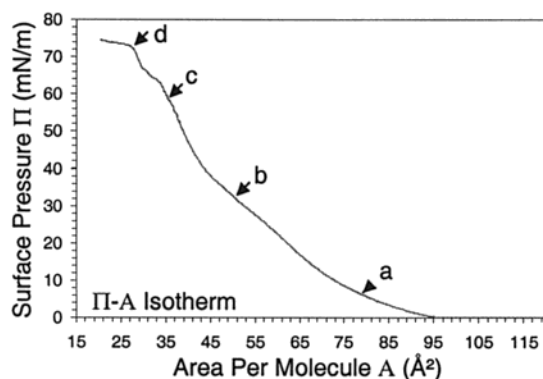*J. Phys. Chem. B, Vol. 105, No. 42, 2001* **10351**

Figure 3. Isotherm for a 7:3 DPPC:POPG monolayer on pure water at 30 °C and FM images taken at various points along the isotherm — (a) the monolayer in a homogeneous LE phase; (b) toward the end of the LE−C coexistence plateau where the dark domains indicate the condensed phase; (c) scattered vesicles (circled) are observed in the biphasic monolayer, this is illustrated by the inset image, which shows a vesicle formed in a 13.75 μm × 13.75 μm region of the monolayer; (d) the collapse of the monolayer is bimodal with both vesicle-like structures (circled) and several hundred micrometer long folds (bright streaks).
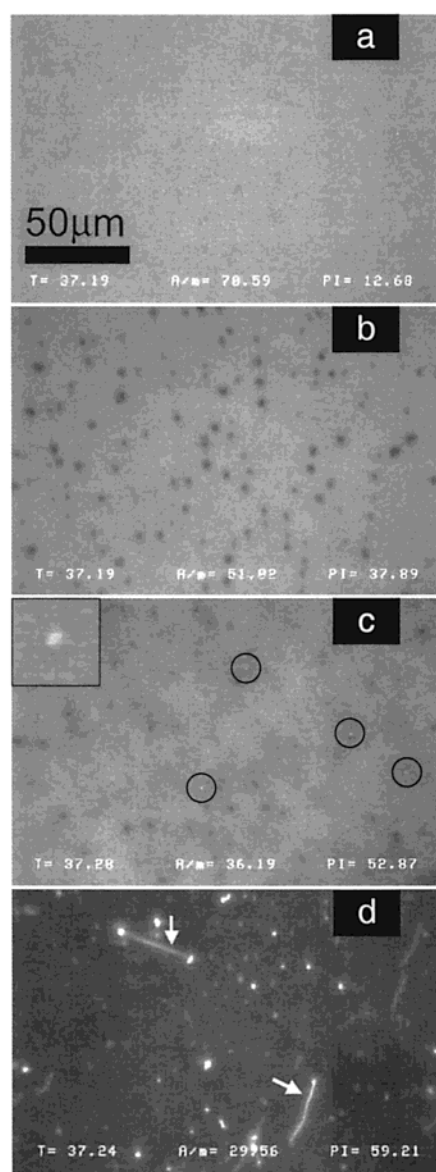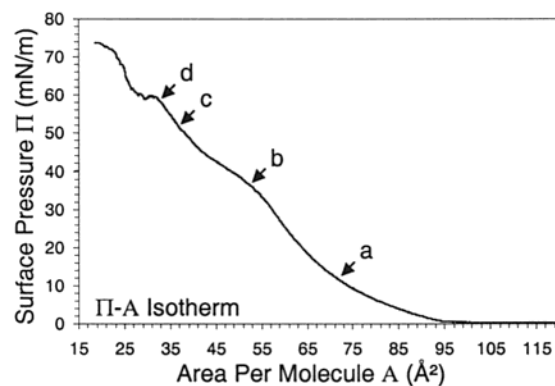

Figure 4. Isotherm for a 7:3 DPPC:POPG monolayer on pure water at 37 °C and FM images taken at various points along the isotherm — (a) the monolayer in a homogeneous LE phase; (b) sometimes, there is slight nucleation of the dark condensed phase; (c) the monolayer becomes homogeneous at higher Π and the nucleation of vesicles (circled) begins; the inset image shows a 13.75 μm × 13.75 μm region of the monolayer where a vesicle has nucleated; (d) most budding vesicles grow large and detach from the monolayer, while some form long fingerlike tubular structures that remain attached to the monolayer (arrows).

The folds were of the order of 100 μm−1 mm long and a few

tens to hundreds of microns wide. Most folds initiated at domain

boundaries between the LE and C phases within approximately 70−100 ms (2−3 video frames) as described elsewhere.[44] The folds, subsequently, propagated very quickly in length (up to millimeters in 30−100 ms) and showed no observable preference for the domain boundaries. Upon releasing the surface pressure by expanding the barriers, these structures unfolded and re-incorporated their material back into the monolayer while retaining most of their original biphasic morphology.

The morphological changes observed upon collapse at 20, 28, and 30 °C were similar to those observed at 25 °C with folding as the primary mode of monolayer collapse. As explained earlier, C phase domains were sometimes observed to nucleate in the presence of G and LE phases at 20 °C (data not presented). At 30 °C, white spots (diameters from 1 to 10 μm), indicating the formation of budding vesicles, were formed at Π between 50 and 55 mN m^{-1} and were seen bound to the monolayer at higher Π (Figure 3c,d). The bright spots did not detach from the monolayer at higher Π and re-incorporated into the monolayer upon expansion. Slight vesiculation (2 or 3 vesicles in a 150 × 220 μm area) was sometimes observed even at 28 °C.

Compression of the uniform LE phase did not lead to significant nucleation of the condensed phase at temperatures above 33.5 °C. On rare occasions, we observed nucleation of the condensed phase (Figure 4c) at temperatures up to 37 °C, but the monolayer became homogeneous upon further compression and remained so until collapse occurred. These nucleation events were probably caused by local compositional inhomogeneity of the film. Collapse proceeded by nucleation of vesicles at Π between 45 and 55 mN m^{-1} and their subsequent detachment. Two types of vesicles were observed: 1−10 μm globular structures and tubular fingerlike structures attached at one end to the monolayer and dangling into the water subphase at the other (Figure 4d). Globular vesicles typically detached from the monolayer and diffused into the bulk of the subphase upon further compression; the ones that remained associated with the monolayer re-incorporated upon expansion. Tubular vesicles always remained attached to the monolayer and re-incorporated into the monolayer upon expansion. Although detailed structure for either type of vesicle is not known, height profiles obtained from preliminary atomic force microscopy (AFM) studies of monolayers deposited on mica substrates using methods described elsewhere[21] indicate that the bright spots observed forming from the monolayer are most probably unilamellar vesicles.

The Π−T Phase Diagram. Since the formation of folds and vesicles attached to the monolayer is reversible upon expansion, we have drawn the equivalent of a pressure−temperature phase diagram for these 2D−3D transitions (Figure 5). In this quasi-phase diagram, the nucleation pressures (Π) of the folding transitions (squares) and vesicle formation (diamonds) are plotted against their corresponding temperatures (*T*). The diagram indicates a first-order-like transition between the two collapse modes modulated by temperature. To investigate if these collapse modes could be thought of as equilibrium "phases", we attempted to find the equivalent of a "triple point" for this system of 2D−3D transitions. In this scheme, a "triple point" would be a combination of Π and *T* at which the 2D monolayer would coexist with folds as well as budding vesicles. At 30 ˚C (Figure 3d), and occasionally at 28 ˚C, the monolayer exhibits both vesicles and folds in equilibrium with the parent monolayer. Above 33.5 ˚C the monolayer is in the uniform LE phase and collapses only by vesiculation. This suggests that the
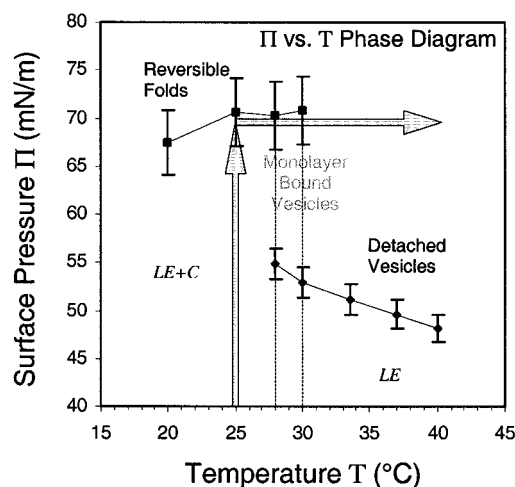

Figure 5. Surface pressure (Π) vs temperature (*T*) phase diagram − the squares (■) indicate the point of nucleation of the folding transition and the diamonds (◆) indicate the point of abrupt increase in budding of vesicle-like structures. The vertical and horizontal arrows indicate the isothermal compression and heating of the monolayer, respectively, during the heating experiment.

postulated "triple point" for the fold−vesicle transition, if present, lies between 28 and 33.5 °C for this lipid system.

Heating Experiments. If the folding−vesiculation transition predicted by the Π−*T* phase diagram is a first-order transition, the collapse mode should be independent of the path taken to attain that state. To test the path dependence of the current system, we conducted a heating experiment. The arrows in Figure 5 indicate the path. For this lipid system, folding occurs at high Π and vesicle formation at low Π. It is therefore necessary that the measurement begins in the folding state and then transforms via heating to the vesiculating state. The reverse experiment involving cooling cannot work because vesiculation always occurs at surface pressures lower than those at which folds form (see Figure 5). In addition, vesiculation involves the rapid loss of material from the surface, making the maintenance of constant Π impractical, and causing alterations in the monolayer lipid composition during the experiment.

In all the heating experiments performed, the monolayer, at an initial temperature of 25 °C, was first compressed until folding occurred. At this point the trough assembly including the water subphase was heated while holding Π constant. The heating experiments were performed until the barriers hit their compression limit. Several such heating experiments were made at the same heating rate to ascertain reproducibility. A representative series of monolayer morphology images is presented in Figure 6.

On heating a folded monolayer (Figure 6a) from 25 to 40 °C, the first visible event occurred between 30 and 33.5 °C where there was an abrupt formation of a large number of vesicles at the LE−C domain boundaries in both the monolayer and the 3D folded region (Figure 6b). Above 33.5 °C, the vesicular collapse mode became predominant (Figure 6c), and vesicles grew and detached from both the folds and the monolayer (Figure 6d). Some of the vesicles fused with each other to form larger ones before they detached from the folded region (Figure 6d).

Discussion and Conclusions

Temperature-Modulated 2D−3D Transition. Our results show that the mode by which monolayers composed of 7:3 DPPC:POPG collapse at the air−water interface can be controlled by temperature.
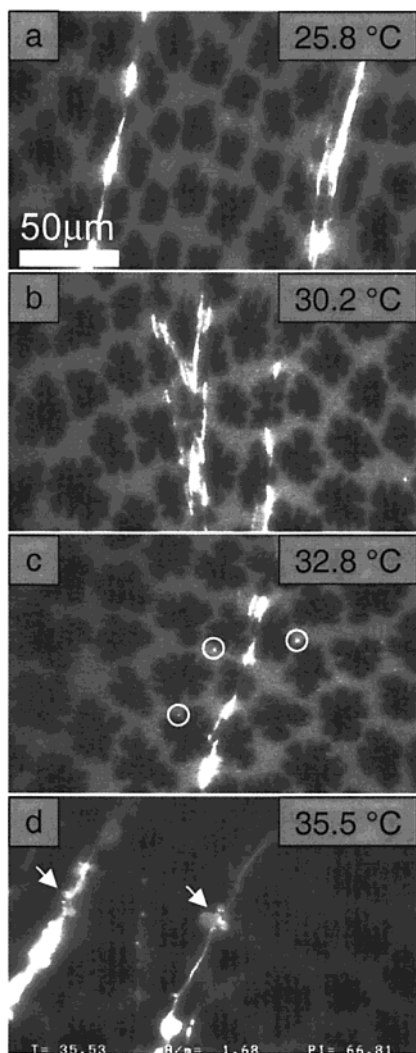
Figure 6. Fluorescence micrographs of a 7:3 DPPC:POPG monolayer at different temperatures during the heating experiment. (a) At 25.8 °C, the predominant collapse structures observed are folds. The monolayer shows a few vesicles (white spots) along with folds, but they are not significant in number. (b) At 30.2 °C, the monolayer does not show any considerable change from the previous image at a lower temperature. (c) At 32.8 °C, the monolayer shows a large number of vesicles being formed at the boundaries between the condensed (dark) and disordered (gray) phases. This abrupt increase in the number of vesicles normally starts between 31 and 33 °C. Beyond 33 °C, the vesicles bound to the monolayer or the folded region either fuse to form larger ones or detach and diffuse into the subphase. (d) At 35.5 °C, the region in focus shows the formation of vesicles from the folds below the plane of the monolayer. The arrows indicate regions where smaller vesicles have fused to form larger ones.

At temperatures below 30 °C, the condensed domains are larger than those at higher temperatures and equivalent Π, and occupy a larger area fraction of the monolayer. When compressed further, the biphasic monolayer buckles into folds up to several hundred micrometers wide and several millimeters long. Recent work[56] indicates that mixed monolayers of lung surfactant phospholipids tend to remain phase separated at high compression. The differences in headgroup charge and acyl chains lead to separation of the monolayer into two phases of different chemical compositions.[47,48,57] In the 7:3 DPPC:POPG monolayer used here, the condensed phase is DPPC-rich, while the disordered phase at high surface pressures is POPG-rich.

Above 30 °C, monolayers of identical composition collapse by budding and detachment of micrometer scale 3D structures from the monolayer. Ejection of materials from the monolayer into the subphase has been previously reported as a mode of collapse.[58] These 3D structures are expected to be composed of lipid bilayers,[59] and our preliminary AFM studies of transferred monolayers suggest that they are likely to be unilamellar vesicles. Comparing FM images of the lipid monolayer at similar areas per molecule but different temperatures (Figures 2b, 3b, and 4b) indicates that the increase in temperature changes the morphology of the monolayer prior to collapse. The condensed phase domains, present in the monolayer just prior to collapse, decrease in size and area coverage from 20 to 33.5 °C. This change can be viewed as a thermally driven increase in miscibility between the two components, which in turn leads to change in local composition, morphology, and other mechanical properties. The collapse behavior of the monolayer changes as it is driven thermally from a phase-separated to a homogeneous state above 33.5 °C. Therefore, our results suggest a correlation between monolayer morphology and collapse behavior. This observation is supported by the fact that folding transitions have been seen in monolayers of other compositions, and notably, two-phase coexistence had always been observed before the monolayer buckled.[35,58] Thus, the morphology of the monolayer at collapse seems to determine its mode of 2D−3D transition on further compression.

Morphological Dependence Model for Collapse. To explain this possible correlation between the monolayer morphology and its collapse mode, it is necessary to understand how microscopic quantities such as the spontaneous curvature and rigidity of the phases can affect the topography of the monolayer and thus its collapse behavior. Our studies show that folding or vesiculation in biphasic monolayers originates mostly at the boundary between the LE phase and C domains[44] and any monolayer that collapses via folding is able to sustain high surface pressures (Figure 5). On the basis of these observations, we have developed a theoretical model for biphasic monolayers which has been discussed in detail elsewhere.[43,44] Qualitatively, the model suggests that whenever there are two phases in coexistence, the difference in spontaneous curvature and rigidity of the two phases induces the formation of slightly elevated "mesas". The boundaries between the condensed and the fluid phases are the locations where the monolayer is inflected and therefore the natural locations for nucleation of collapse. The propensity of the 7:3 DPPC:POPG monolayer to sustain high pressures or to form large folded 3D structures, according to this model, stems from its biphasic mesa topography and the mechanical properties associated with such a system. At temperatures above 30 °C, the increase in the amount of disordered phase is associated with a corresponding increase in the fluidity (or reduction in rigidity) of the film. Hence, the less rigid monolayer may not be able to sustain large-scale folding, and collapses on a smaller length scale by forming vesicle-like structures.

Collapse Phase Transition. The transition between the folding and vesiculation collapse modes resembles an equilibrium first-order phase transition. The three-phase coexistence of flat, folded, and vesiculated regions lies between 28 and 33.5 °C. The phase transition is coupled to the change in the morphology of the film. The morphology of the film, whether biphasic or homogeneous, is governed by the temperature of the experiment. The transition from a phase-separated to a homogeneous film for this system takes place at a temperature between 30 (Figure 3) and 33.5 °C (similar to Figure 4). This temperature range coincides with that in which the "triple point" for the collapse mode transition lies.

Tubular Vesicles. Monolayers at or above 33.5 °C are in the homogeneous LE phase at collapse and exhibit vesiculation with the formation of long fingerlike tubular collapse structures (Figure 4b). These structures sometimes grow into the subphase and can get as long as 175 μm. These structures bear resemblance to key features of a collapse mode proposed by Hu and Granek.[42] They argue that in a uniform monolayer with a nonzero spontaneous curvature and below a critical surface tension, a hexagonal array of long fingerlike tubes is favored over a flat surface. While fingering collapse structure is unlikely for single-component systems, the presence of more than one component in the monolayer might, in their opinion, help stabilize the tubular structure. Perhaps a homogeneous binary lipid mixture such as 7:3 DPPC:POPG above 33.5 °C may nucleate and sustain such fingerlike tubular structures as products of collapse.

Application to Lung Surfactant. Monolayers of lung surfactant lipid extracts remain phase separated at high Π near 37 °C.[46] Though the 7:3 DPPC:POPG monolayer is a homogeneous LE phase at 37 °C, other lipid and protein components found in natural lung surfactant may induce phase separation; i.e., shift the maximum temperature for phase separation to a value higher than 37 °C. It is important for lung surfactant to attain near-zero surface tension in order to effectively reduce the work of breathing. The folding mode of collapse would allow the lung surfactant to yield gracefully to compression and reduce its projected area while avoiding irreversibility and loss of surfactant. Since the reversible folding transition is shown to require a biphasic monolayer, it might be favorable to maintain a phase-separated structure in the lung surfactant monolayer. Recent work on model lung surfactant lipid mixtures[52,56] and investigation of the effects of proteins and polyelectrolytes on lipid monolayers[52,58,60,61] all seem to support this conjecture.

References and Notes

(1) Möhwald, H. *Ann. Rev. Phys. Chem.* **1990**, *41*, 441.

(2) Zasadzinski, J. A.; Viswanathan, R.; Madsen, L.; Garnaes, J.; Schwartz, D. K. *Science* **1994**, *263*, 1726.

(3) Veldhuizen, R.; Nag, K.; Orgeig, S.; Possmayer, F. *Biochim. Biophys. Acta* **1998**, *1408*, 90.

(4) Greiner, J. V.; Glonek, T.; Korb, D. R.; Booth, R.; Leahy, C. D. *Ophthalmic Res.* **1996**, *28*, 44.

(5) Grace, A.; Kowk, P.; Hawke, M. *Arch. Otolaryngology − Head and Neck Surgery* **1987**, *96*, 336.

(6) Hills, B. A. *Arch. Otolaryngology − Head and Neck Surgery* **1984**, *110*, 3.

(7) Π (Surface Pressure) = $\gamma_o − \gamma$ where γ_o is the surface tension of the air−water interface and γ is the surface tension of the air−water interface in the presence of the monolayer material.

(8) Gaines, G. L., Jr. *Insoluble Monolayers at Liquid−Gas Interfaces*; Interscience Publishers: New York, 1966.

(9) Möhwald, H. *Rep. Prog. Phys.* **1993**, *56*, 653.

(10) Knobler, C. M.; Desai, R. C. *Ann. Rev. Phys. Chem.* **1992**, *43*, 207.

(11) Kaganer, V. M.; Möhwald, H.; Dutta, P. *Rev. Mod. Phys.* **1999**, *71*, 779.

(12) Weis, R. M. *Chem. Phys. Lipids* **1991**, *57*, 227.

(13) Andelman, D.; Brochard, F.; Knobler, C.; Rondelez, F. Structures and phase transitions in Langmuir Monolayers. In *Micelles, Membranes, Microemulsions and Monolayers*; Gelbart, W., Ben-Shaul, A., Roux, D., Eds.; Springer-Verlag New York Inc.: New York, 1994; p 559.

(14) McConnell, H. M. *Ann. Rev. Phys. Chem.* **1991**, *42*, 171.

(15) Bibo, A. M.; Knobler, C. M.; Peterson, I. R. *J. Phys. Chem.* **1991**, *95*, 5591.

(16) Smith, R. D.; Berg, J. C. *J. Colloid Interface Sci.* **1980**, *74*, 273.

(17) Nikomarov, E. S. *Langmuir* **1990**, *6*, 410.

(18) Vollhardt, D. *Adv. Colloid. Interface Sci.* **1993**, *47*, 1.

(19) Morelis, R. M.; Girardegrot, A. P.; Coulet, P. R. *Langmuir* **1993**, *9*, 3101.

(20) Schürch, S.; Green, F. H. Y.; Bachofen, H. *Biochimi. Biophys. Acta* **1998**, *1408*, 180.

(21) Lee, K. Y. C.; Lipp, M. M.; Takamoto, D. Y.; Ter-Ovanesyan, E.; Zasadzinski, J. A.; Waring, A. J. *Langmuir* **1998**, *14*, 2567.

(22) Lipp, M. M.; Lee, K. Y. C.; Zasadzinski, J. A.; Waring, A. J. *Rev. Sci. Instru.* **1997**, *68*, 2574.

(23) Stine, K. J. *Microscopy Res. Technique* **1994**, *27*, 439.

(24) Meunier, J. *Colloids Surf., A − Physicochemical and Engineering Aspects* **2000**, *171*, 33.

(25) Marshall, G.; Dennin, M.; Knobler, C. M. *Revi. Sci. Instrum.* **1998**, *69*, 3699.

(26) Lheveder, C.; Henon, S.; Mercier, R.; Tissot, G.; Fournet, P.; Meunier, J. *Rev. Sci. Instrum.* **1998**, *69*, 1446.

(27) Mobius, D. *Curr. Opin. Colloid Interface Sci.* **1998**, *3*, 137.

(28) Meine, K.; Vollhardt, D.; Weidemann, G. *Langmuir* **1998**, *14*, 1815.

(29) Horiuchi, Y.; Yagi, K.; Hosokawa, T.; Yamamoto, N.; Muramatsu, H.; Fujihira, M. *J. Microscopy* **1999**, *194*, 467.

(30) Knobler, C. M. *Physica A (Amsterdam)* **1997**, *236*, 11.

(31) Zasadzinski, J. A. N.; Woodward, J. T.; Longo, M. L.; Dixon-Northern, B. *ACS Symp. Ser.* **1992**, *493*, 242.

(32) Schief, W. R.; Dennis, S. R.; Frey, W.; Vogel, V. *Colloids Surf., A − Physicochemical and Engineering Aspects* **2000**, *171*, 75.

(33) Schief, W. R.; Touryan, L.; Hall, S. B.; Vogel, V. *J. Phys. Chem. B* **2000**, *104*, 7388.

(34) Ridsdale, R. A.; Palaniyar, N.; Possmayer, F.; Harauz, G. *J. Membr. Biol.* **2001**, *180*, 21.

(35) Lipp, M. M.; Lee, K. Y. C.; Takamoto, D. Y.; Zasadzinski, J. A.; Waring, A. J. *Phys. Rev. Lett.* **1998**, *81*, 1650.

(36) Saint-Jalmes, A.; Gallet, F. *Eur. Phys. J. B* **1998**, *2*, 489.

(37) Angelova, A.; Vollhardt, D.; Ionov, R. *J. Phys. Chem.* **1996**, *100*, 10710.

(38) Vollhardt, D.; Gutberlet, T. *Colloids Surf., A − Physicochemical and Engineering Aspects* **1995**, *102*, 257.

(39) Kato, T.; Matsumoto, N.; Kawano, M.; Suzuki, N.; Araki, T.; Iriyama, K. *Thin Solid Films* **1994**, *242*, 223.

(40) Lundquist, M. *Chem. Scr.* **1971**, *1*, 197.

(41) Kampf, J. P.; Frank, C. W.; Malmstrom, E. E.; Hawker, C. J. *Science* **1999**, *283*, 1730.

(42) Hu, J. G.; Granek, R. *J. Phys. II* **1996**, *6*, 999.

(43) Diamant, H.; Witten, T. A.; Ege, C.; Gopal, A.; Lee, K. Y. C. *Phys. Rev. E* **2001**, *63*.

(44) Diamant, H.; Witten, T. A.; Gopal, A.; Lee, K. Y. C. *Europhys. Lett.* **2000**, *52*, 171.

(45) Brown, D. A.; London, E. *Annu. Rev. Cell Developmental Biol.* **1998**, *14*, 111.

(46) Discher, B. M.; Maloney, K. M.; Schief, W. R.; Grainger, D. W.; Vogel, V.; Hall, S. B. *Biophys. J.* **1996**, *71*, 2583.

(47) Maloney, K. M.; Grainger, D. W. *Chem. Phys. Lipids* **1993**, *65*, 31.

(48) Koppenol, S.; Yu, H.; Zografi, G. *J. Colloid Interface Sci.* **1997**, *189*, 158.

(49) Discher, B. M.; Schief, W. R.; Vogel, V.; Hall, S. B. *Biophys. J.* **1999**, *77*, 2051.

(50) Bagatolli, L. A.; Gratton, E. *Biophys. J.* **2000**, *78*, 1051Pos.

(51) Muresan, A. S.; Diamant, H.; Lee, K. Y. C. *J. Am. Chem. Soc.* **2001**, *123*, 6951.

(52) Nag, K.; Munro, J. G.; Inchley, K.; Schurch, S.; Petersen, N. O.; Possmayer, F. *Am. J. Physiol.−Lung Cellular Molecular Physiology* **1999**, *277*, L1179.

(53) Boonman, A. A. H.; Snik, A.; Egberts, J.; Demel, R. *Prog. Respiratory Res.* **1984**, *18*, 18.

(54) Vargaftik, N. B.; Volkov, B. N.; Voljak, L. D. *J. Phys. Chem. Ref. Data* **1983**, *12*, 817.

(55) Ruckenstein, E. *J. Colloid. Interface Sci.* **1997**, *196*, 313.

(56) Crane, J. M.; Putz, G.; Hall, S. B. *Biophys. J.* **1999**, *77*, 3134.

(57) Dorfler, H. D.; Koth, C.; Rettig, W. *J. Colloid Interface Sci.* **1996**, *180*, 478.

(58) Takamoto, D. Y.; Lipp, M. M.; von Nahmen, A.; Lee, K. Y. C.; Waring, A. J.; Zasadzinski, J. A. *Biophys. J.* **2001**, *81*, 153.

(59) Seifert, U. *Adv. Phys.* **1997**, *46*, 13.

(60) deMeijere, K.; Brezesinski, G.; Möhwald, H. *Macromolecules* **1997**, *30*, 2337.

(61) Kruger, P.; Schalke, M.; Wang, Z. D.; Notter, R. H.; Dluhy, R. A.; Losche, M. *Biophys. J.* **1999**, *77*, 903.